Steady-State Kinetic Investigation of Cytochrome P450cam: Interaction with Redox Partners and Reaction with Molecular Oxygen†

Matthew M. Purdy,‡ Laura S. Koo,§ Paul R. Ortiz de Montellano,§ and Judith P. Klinman*,‡,||

Department of Chemistry and Department of Molecular and Cell Biology, University of California, Berkeley, California 94720-1460, and Department of Pharmaceutical Chemistry, University of California, San Francisco, California 94143-2280

Received September 5, 2003

ABSTRACT: Cytochrome P450cam (CYP101) is a prokaryotic monooxygenase that requires two proteins, putidaredoxin reductase (PdR) and putidaredoxin (Pdx), to supply electrons from NADH. This study addresses the mechanism by which electrons are transported from PdR to P450cam through Pdx and used to activate O_2 at the heme of P450cam. It is shown that $k_{cat}/K_m(O_2)$ is independent of the PdR concentration and hyperbolically dependent on Pdx. The phenomenon of saturation of reaction rates with either P450cam or PdR at high ratios of one enzyme to the other is investigated and shown to be consistent with a change in the rate limiting step. Either the reduction of Pdx by PdR (high P450) or the reduction of P450 by Pdx (high PdR) determines the rate. These data support a mechanism where Pdx acts as a shuttle for transport of electrons from PdR to P450cam, effectively ruling out the formation of a kinetically significant PdR/Pdx/P450cam complex.

The mechanism of the camphor hydroxylating enzyme cytochrome P450cam (CYP101) from *Pseudomonas putida* has been extensively studied (*1*, *2*). The goal of the present work is to examine the early steps in O_2 activation that lead to the formation of the terminal oxidant and substrate hydroxylation. The nature of several oxygen bound intermediates in the catalytic cycle has been investigated by spectroscopic (*3*−*6*), theoretical (*7*, *8*), and stopped-flow kinetic methods (*5*, *9*−*13*). However, with some notable exceptions (*14*, *15*), few detailed steady-state kinetic studies have been published with P450cam. This is not surprising due to the complexity derived from the need for two redox partners to supply electrons. The flavoprotein putidaredoxin reductase (PdR)[1] accepts two electrons from NADH. One at a time, these electrons are transferred to cytochrome P450cam through the mediation of the $[Fe_2S_2]$ protein putidaredoxin (Pdx). Scheme 1 depicts the flow of electrons from NADH to P450cam, illustrating the requirement for two single electron transfers from Pdx to P450cam during catalysis. The first electron transfer reduces P450cam to the ferrous form so that it may bind O_2. The second transfer reduces this oxygen bound form, formally an Fe(III)−superoxide complex, to an Fe(III)−peroxide complex.

Three possible mechanisms for the flow of electrons from PdR to P450cam are the cluster, Pdx shuttle, and transient cluster mechanisms. The terms shuttle (*16*) and cluster (*17*) mechanism come from the literature of the adrenal gland steroid hydroxylase, a mitochondrial P450 that is similar to P450cam in its use of an $[Fe_2S_2]$ containing adrenodoxin and flavoprotein adrenodoxin reductase as analogues of Pdx and PdR, respectively. Similar mechanistic issues are under debate in the P450cam and steroid hydroxylase systems (*1*). In a cluster mechanism, a PdR/Pdx/P450cam complex forms and survives for one or more turnovers. This would indicate that both electrons from one molecule of NADH move through the flavin of PdR to sequentially reduce the same Pdx and P450cam molecules. In contrast, a shuttle mechanism does not require a complex of all three proteins during the catalytic cycle, involving the reduction of Pdx^{ox} by PdR and release of the reduced form of putidaredoxin (Pdx^r) into solution. In a subsequent step, Pdx^r binds to and reduces P450cam. A third mechanism, the transient cluster mechanism, is a hybrid of the other two. Here, a single molecule of Pdx remains bound to the P450cam throughout one or more catalytic cycles. The cycling of Pdx^{ox} to Pdx^r occurs via a transient association of fully reduced or one-electron reduced PdR to the Pdx^{ox}/P450cam complex.

Evidence in support of the shuttle mechanism includes the ability of PdR to reduce Pdx in the absence of P450cam (*15*, *18*) and of Pdx^r to carry out both of the electron transfer steps to P450cam in the absence of PdR (*9*−*12*, *19*). Additionally, mutagenesis studies of surface residues have indicated partial overlap of the proposed binding sites on Pdx for PdR and P450cam (*20*), suggesting that PdR and P450cam cannot bind simultaneously to Pdx. However, other

† This work was supported by National Institutes of Health Grants GM 25765 (J.P.K.) and GM 25515 (P.R.O.M.). M.M.P. was supported in part by a National Institutes of Health Biophysics Pre-Doctoral Training Grant (5 T32 GM 08295-13).

* To whom correspondence should be addressed. Phone: (510) 642-2668. Fax: (510) 643-6232. E-mail: klinman@socrates.berkeley.edu.

‡ Department of Chemistry, University of California, Berkeley.

§ University of California, San Francisco.

|| Department of Molecular and Cell Biology, University of California, Berkeley.

[1] Abbreviations: P450cam, cytochrome P450cam (CYP101); PdR, putidaredoxin reductase; Pdx, putidaredoxin; Pdx^r, the reduced form of putidaredoxin; Pdx^{ox}, the oxidized form of putidaredoxin; $PdR^{r/s}$, putidaredoxin reductase in either the two- or one-electron reduced form; $PdR^{s/ox}$, putidaredoxin reductase in either the one-electron reduced or fully oxidized form; IPTG, isopropyl-*β*-D-thiogalactopyranoside; *β*ME, 2-mercaptoethanol; MOPS, 3-(*N*-morpholino)propanesulfonic acid; DTT, dithiothreitol.

10.1021/bi0356045 CCC: $27.50
Published on Web 12/12/2003

Scheme 1: Electron Transport from PdR to P450cam Mediated by Pdx

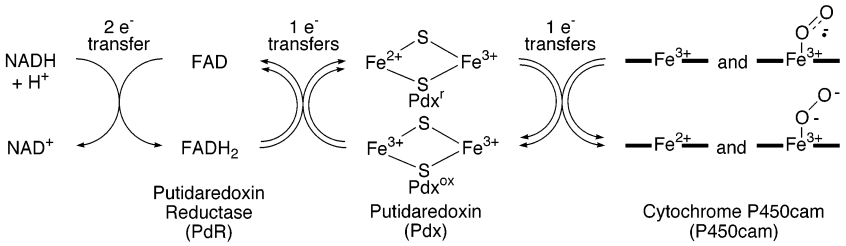

experimental results also exist that may implicate a functional ternary complex of P450cam, PdR, and Pdx. For example, a fusion protein of PdR, Pdx, and P450cam has been shown to turn over efficiently (*21*), and calorimetric studies indicate different contributions of hydrophobic, electrostatic, and hydrogen bonding interactions for a Pdx/P450cam complex than a Pdx/PdR complex (*22*). Using Pdx immobilized on a surface, the formation of a three-enzyme complex has been demonstrated that is predicted to have a sufficient lifetime for 60 catalytic turnovers (*23*). Clearly, more definitive studies are needed to distinguish a shuttle from a cluster mechanism.

In the present work, steady-state kinetics are applied to investigate the delivery of electrons to P450cam in the early steps of O_2 activation. Previous studies have examined the effect of variation of the concentrations of Pdx and PdR on the rates of reaction of P450cam (for a few examples, see refs *14*, *20*, and *24*). Here, variation of the concentration of O_2 is carried out for the first time, to examine the kinetic parameter $k_{cat}/K_m(O_2)$. It is shown that evaluation of this parameter at multiple concentrations of Pdx and PdR can provide unique information regarding catalytic complex formation between P450cam, O_2, and the redox partner being varied. The availability of $k_{cat}/K_m(O_2)$ also allows comparison to a previously measured value for the rate for O_2 binding to ferrous P450cam, suggesting at least one kinetically significant step beyond the formation of the enzyme$-O_2$ complex. Finally, these data provide values for the apparent $K_m(O_2)$ at different concentrations of Pdx and PdR. In general, the reaction of P450cam has been studied at one O_2 concentration (air saturation), with a single rough estimate of $K_m(O_2)$ for P450cam (*25*) coming from a progress curve under one set of Pdx and PdR concentrations. Knowledge of $K_m(O_2)$ establishes conditions for kinetic saturation with O_2 and allows estimation of true k_{cat} values.

EXPERIMENTAL PROCEDURES

Materials. MOPS, DTT, NADH, and horse heart cytochrome *c* (type VI) were obtained from Sigma. Cytochrome *c* was dialyzed against the assay buffer before use. Sephacryl S-100 and fast-flowing Q Sepharose resins were purchased from Amersham Pharmacia. (1*R*)-(+)-Camphor was a product of Aldrich and was delivered to buffers from a 1 or 2 M stock solution in ethanol.

Preparation of Enzymes. P450cam was expressed as an N-terminal $(His)_6$ fusion protein as previously described (*26*). To eliminate the presence of any disulfide cross-linked P450cam dimer (*27*), a solution of approximately 250 μM P450cam was incubated with 30 mM DTT at 30 °C for 30 min. To remove the DTT, the reaction mixture was then passed over a Sephadex G-25 column equilibrated with pH 7.4, 50 mM MOPS-KOH buffer with 69 mM KCl and 0.3−1 mM camphor. Colored elutant fractions were collected and diluted to 2−30 μM in P450cam as determined by the Soret band absorbance of the ferric, camphor bound form at 391 nm using $\epsilon = 102$ mM^{-1} cm^{-1} (*28*). The solution was either used immediately or frozen in aliquots and stored at −80 °C. Each aliquot was thawed only once and used within 12 h. No dimerized P450cam was detected in the thawed aliquots by nonreducing SDS−PAGE.

The wild type P450cam, used for comparison to the $(His)_6$ tagged protein, was expressed in *Escherichia coli* as described previously (*29*). The $(His)_6$ tagged P450cam was used in all experiments except those where the wild type is explicitly mentioned.

Putidaredoxin was expressed in *E. coli* strain DH5α using the plasmid pCWori by the method described by Sibbesen et al. for the P450cam-PdR-Pdx fusion protein (*21*). Frozen cell paste was resuspended in 50 mM Tris-Cl pH 7.4 buffer containing 50 mM KCl, 1 mM EDTA, 5 mM βME, and 200 μM phenylmethanesulfonyl fluoride at room temperature. The remaining steps were carried out at 4 °C. The cells were lysed with lysozyme followed by sonication. After centrifugation, the supernatant was subjected to ammonium sulfate precipitation. The material that precipitated between 40 and 60% ammonium sulfate saturation was collected and then dialyzed against 50 mM Tris-Cl pH 7.4 buffer containing 10 mM βME. Anion exchange chromatography was carried out on a 2.5 × 20 cm (diameter × length) fast-flowing Q sepharose column with a 0−400 mM KCl gradient. After concentration by ultrafiltration using an Amicon YM-3 or YM-10 membrane, the sample was split into two or three portions. These aliquots were either used directly or stored at −80 °C and thawed prior to further purification. Each portion was subject to size exclusion chromatography on a 2.5 × 110 cm Sepharcyl S-100 column with 50 mM MOPS-KOH, 100 mM KCl pH 7.4 buffer containing 10 mM βME. After chromatography, the 10 mM βME was exchanged with 2 mM DTT by several rounds of dilution with 2 mM DTT containing 50 mM MOPS-KOH, 100 mM KCl pH 7.4 buffer followed by concentration by ultrafiltration. The final solution was concentrated to 0.8−1.8 mM Pdx and stored in aliquots at −80 °C. The purified Pdx had an A_{415}/A_{280} of 0.48, comparable to the literature value of 0.49 (*28*). The concentration of Pdx was determined as the average concentration calculated from the two wavelengths 415 and 455 nm using the extinction coefficients 11.1 and 10.4 mM^{-1} cm^{-1}, respectively (*28*).

PdR was expressed and purified as described (*30*), except cells were grown at 37 °C and the temperature lowered to 30 °C only after induction with IPTG. Additionally, the initial ammonium sulfate cut was to 35% saturation. The concen-

tration of PdR was determined as the average of the concentration calculated from each of the three wavelengths 378, 454, and 480 nm using the extinction coefficients 9.7, 10.0, and 8.5 mM^{-1} cm^{-1}, respectively (*28*).

Enzyme Assays. Reactions were followed by O_2 consumption on a Clark-type electrode from Yellow Springs Inc. in a 1 mL final volume at 25 °C containing 50 mM MOPS titrated to pH 7.4 with KOH, 69 mM KCl, and 500 μM camphor. This gave an ionic strength and total concentration of potassium ion equal to 0.1 M. DTT was added to 100 μM final concentration followed by PdR (0.01−3 μM) and Pdx (0.1−15.0 μM). The addition of NADH (500 μM) began the background consumption of O_2 due to the reaction of the reduced forms of both Pdx and PdR with O_2. This background rate was recorded for 2−2.5 min. The reaction was then initiated by the addition of P450cam (8−30 nM). For experiments in which the concentration of P450cam was varied, this concentration range was expanded to 2−70 nM. The concentrations of P450cam employed here are much lower than the 0.5−1 μM typically employed in activity assays. The low concentrations of P450cam were required to slow the rate of the reaction enough to follow the consumption of the O_2 substrate at concentrations near and below its K_m. The low P450cam concentration necessitates a much higher ratio of Pdx to P450cam than typically employed in other studies to saturate the enzyme with this redox partner (*14*). The net enzymatic rate was determined by subtraction of the background rate prior to the P450cam addition from the rate measured after P450cam addition. The inclusion of either DTT or superoxide dismutase was required to protect the Pdx from inactivation due to the production of reactive oxygen species during recording of the background. Reactions were performed at either air saturation or under a mixture of O_2 and N_2 gases to vary the initial O_2 concentration. The concentration of O_2 in solution at 25 °C under air saturation was taken to be 258 μM.

This method of recording background rates has a tendency to overestimate the background contribution at low concentrations of PdR. This is due to more of the Pdx being in the reduced, O_2 reactive form before the addition of P450cam than after. This problem disappears at higher ratios of PdR to P450cam, where the Pdx is maintained in the same reduced form during turnover as during the recording of the background rate. The conventional method of initiating reactions with NADH and recording background rates separately in the absence of P450cam suffers from the same drawback. The rates of the background reaction in the absence of P450cam were typically 5−15% of the total rate of O_2 consumption, and inaccuracies due to overestimation of the background are expected to be minimal. In a few cases with very slow enzymatic reactions, at concentrations of Pdx less than 0.2 μM or PdR less than 10 nM, the background contribution to the total rate was as much as 25%.

Data Analysis. For experiments in which only one substrate or protein concentration was varied, the data were fitted to the Michaelis−Menten equation using the program Kaleidagraph by Synergy Software. For the series of experiments in which the concentration of O_2 was varied at multiple concentrations of Pdx with saturating PdR, the data were fitted by nonlinear least squares regression using the program Mathematica (Wolfram Research) to the equation for a ordered sequential mechanism (*31*), given as eq A.2 in the Appendix, where substrates A and B are Pdx and O_2 respectively, and E is P450cam. As prescribed by Cleland (*32*), for data that include rates that vary by more than a factor of 10, the fitting was carried out by taking the common logarithm of both sides of the equation. To determine the concentration of PdR required for saturation in these experiments, the concentration of PdR was varied at air saturation for each pair of P450cam and Pdx concentrations employed. This provides $[PdR]_{halfmax}$, the concentration of PdR where the rate is half-maximal. The saturating concentration of PdR was taken to be 5−30 (typically 10) times $[PdR]_{halfmax}$. In certain instances, the $[PdR]_{halfmax}$ was interpolated from measurements at other concentrations of Pdx (e.g., at concentrations of Pdx in Figure 2 that are absent from the tables).

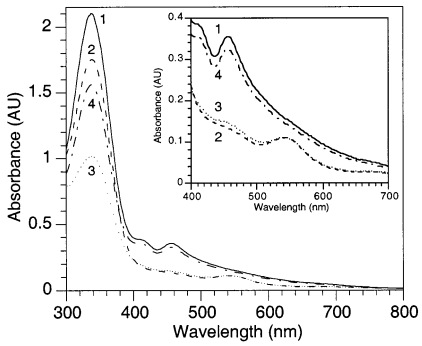

FIGURE 1: Steady-state spectrum of putidaredoxin. To verify that the kinetically saturating concentration of 230 nM putidaredoxin reductase (PdR) was enough to maintain all of the putidaredoxin (Pdx) in its reduced form during turnover at 20 nM P450cam, spectra were taken during a reaction containing 30 μM Pdx. (1) The spectrum of the resting, oxidized Pdx with peaks at 415 and 455 nm was taken after the addition of 0.25 mM NADH (340 nm peak) (—). (2) PdR was added and allowed to reduce the Pdx for 100 s (- - -). Reduction of Pdx is indicated by diminution of the 415 and 455 nm absorbances and formation of a new peak at 545 nm. (3) P450cam was added, and the spectrum was taken after 100 s when approximately two-thirds of the NADH was consumed as indicated by the decrease in absorbance at 340 nm (···). (4) In a separate experiment, 40 nM P450cam and a subsaturating amount of PdR (5 nM) were employed. A spectrum was taken 100 s after P450cam addition when approximately one-third of the NADH was consumed (- · -). Conditions were 25 °C, pH 7.4, 50 mM MOPS-KOH, 69 mM KCl, 0.5 mM camphor, and atmospheric oxygen. Inset: magnification of the 400−700 nm region of the above spectra.

A Scatchard analysis (*33*) was carried out for binding of PdR to P450cam on the assumption that PdR and P450cam form an essential and reversible complex during the catalytic turnover:

$$PdR + P450 \rightleftharpoons PdR{\cdot}P450 \qquad (1)$$

This PdR·P450 complex would likely be bridged by Pdx, which was present in a large excess over both PdR and P450cam in these experiments. The equilibrium constant is given by

$$K_{eq} = [PdR{\cdot}P450]/([PdR][P450]) \qquad (2)$$

where [PdR] and [P450] are the free concentrations of PdR and P450cam, respectively. By rearranging eq 2 and substituting a mass balance relation for the free P450cam concentration of $[P450] = [P450]_{tot} - [PdR{\cdot}P450]$, eq 3

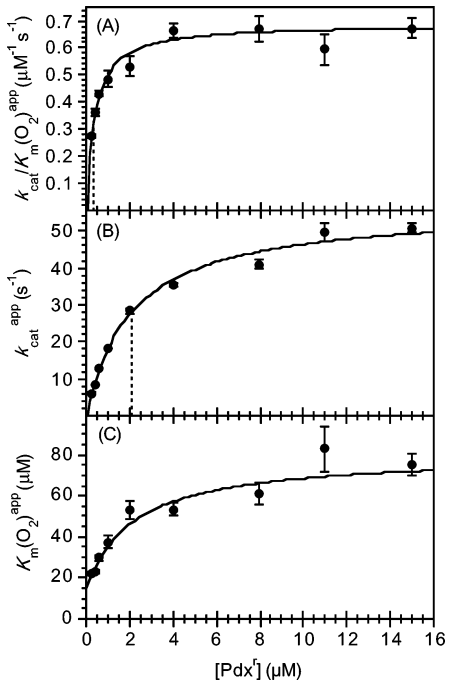

FIGURE 2: O_2 variation at fixed concentrations of Pdx. Parameters were measured with saturating putidaredoxin reductase under conditions as in Table 1. Each point represents the apparent $k_{cat}/K_m(O_2)$ (A), k_{cat} (B), or $K_m(O_2)$ (C) measured by variation of O_2 concentration followed by least-squares fitting to the Michaelis−Menten equation; the error bars represent the standard error in the initial curve fit. The curves shown in all three panels are error weighted fits of the data to a hyperbola. Panels A and B are fit to $y = ax/(b + x)$. The curve in panel C is fit to $y = (a + bx)/(c + x)$ (*34*). The dotted vertical lines in panels A and B represent the concentration of Pdx^r where the parameter is half of its maximal value.

results in

$$[\text{PdR}\cdot\text{P450}]/[\text{PdR}] = K_{eq}[\text{P450}]_{tot} - K_{eq}[\text{PdR}\cdot\text{P450}] \quad (3)$$

A plot of the concentration of the complex divided by the concentration of free PdR versus the concentration of the complex gives a slope of $-K_{eq}$ (*33*). In the version of the plot employed here, the *x*-intercept equals the total P450cam concentration used in the experiment, provided that the binding stoichiometry is 1:1. Since the concentrations of PdR and P450cam used in these experiments are very close to each other, the assumption that $[\text{PdR}] = [\text{PdR}]_{tot}$ cannot be made. The concentrations of [PdR·P450] and [PdR] were, thus, determined as described here. On the assumption of a binding model, the parameter [PdR·P450] was obtained from the ratio of the observed to maximal velocities, eq 4, with V_{max} being determined at each $[\text{P450}]_{tot}$ by a fit to the Michaelis−Menten equation for changing PdR concentrations and extrapolation to saturating PdR. In the latter case, concentrations of PdR were kept high in relation to $[\text{P450}]_{tot}$.

$$[\text{PdR}\cdot\text{P450}] = [\text{P450}]_{tot}\upsilon_{obs}/V_{max} \quad (4)$$

By difference, the concentration of unbound PdR is

$$[\text{PdR}] = [\text{PdR}]_{tot} - [\text{PdR}\cdot\text{P450}] \quad (5)$$

Spectrum of Pdx During Steady State. The UV−vis spectrum of Pdx during turnover was recorded on a Hewlett-Packard 8452A diode array spectrophotometer. The reaction conditions were the same as described for O_2 consumption assays, except that no DTT was added, the concentration of NADH was 250 μM, and wild type P450cam was used. First, the spectrum of a mixture of NADH and oxidized Pdx was determined in the reaction buffer. PdR was added and allowed to reduce the Pdx for 100 s. A spectrum was recorded to verify complete reduction of the Pdx. P450cam was then added, and the UV−vis spectra were recorded at 10 s intervals. The enzyme concentrations used in this experiment were 30 μM Pdx, 20 nM P450cam, and 0.23 μM PdR.

Cytochrome c Reduction Assay. The rate of transfer of electrons from PdR to Pdx was determined by using an excess of the alternate electron acceptor, cytochrome *c*, in place of P450cam (*15*, *18*). Assays were performed under the same conditions as O_2 consumption, except concentrations were changed to 4 μM DTT and 250 μM NADH. The enzyme concentrations were 12.5 nM PdR, 4.0 μM Pdx, and 30 μM cytochrome *c*. Reactions were initiated by NADH and followed by the increase in absorbance at 550 nm using a Varian Cary 3B spectrophotometer. Absorbance changes were converted to concentration changes using 21 mM^{-1} cm^{-1} as the difference in extinction coefficients between the reduced and the oxidized forms of cytochrome *c* (*21*). The rate reported in the text of the Results section is the average of three measurements.

RESULTS

Determination of Concentrations of PdR Required for Saturation. In sets of reactions where it was necessary to maintain Pdx in its reduced form during turnover, a large excess of PdR over P450cam was required. The amount needed was determined by a variation of the concentration of PdR at each pair of P450cam and Pdx concentrations to be employed in further experiments. The plots of rate versus concentration of PdR at fixed P450cam and Pdx concentrations were hyperbolic and could be fit to the Michaelis−Menten equation to give the values for the apparent V_{max} and $[\text{PdR}]_{halfmax}$ shown in Tables 1 and 3A. The $[\text{PdR}]_{halfmax}$ is the concentration of PdR required to obtain half of the maximal rate. It is not referred to as a K_m because it is unlikely that PdR binds to the P450cam enzyme during the catalytic cycle (see below).

At a constant concentration of Pdx, the values of $[\text{PdR}]_{halfmax}$ increase linearly with the concentration of P450cam as shown in Table 3A. This is attributed to the need for more PdR to maintain Pdx in its reduced state under conditions of an increased rate of Pdx oxidation by P450cam. When P450cam is kept constant, the concentration of PdR required to saturate the system increases with decreasing concentrations of Pdx (Table 1). This effect can be explained by the observation that the reaction between PdR and Pdx is nearly second order at the concentrations employed in this study. Roome and Peterson reported that PdR has a K_m(Pdx) of 140 μM using cytochrome *c* as an alternate electron acceptor in place of P450cam (*15*). Under the conditions of the present study, where the concentration of Pdx was $\leq$15 μM, a nearly linear dependence of the rate on [Pdx] during its reduction by PdR was confirmed using the cytochrome *c* reduction assay (data not shown).

The PdR variation experiments were, in general, performed under the atmospheric concentration of O_2 for convenience.

Table 1: Results of PdR Variation Experiments[a]

(A) 13 nM P450cam

[Pdx] (μM)	$[PdR]_{halfmax}$ (nM)	apparent V_{max} (μM O_2/min)
1.0	61 ± 6	14.7 ± 0.5
4.0	25 ± 3	28 ± 1
4.0[b]	29 ± 4	33 ± 1
8.0	16 ± 2	34 ± 2
8.0[c]	25 ± 3	41 ± 2
15.0	8 ± 1	35 ± 1

(B) 31 nM P450cam

[Pdx] (μM)	$[PdR]_{halfmax}$ (nM)	apparent V_{max} (μM O_2/min)
0.20	200 ± 20	10.9 ± 0.3
0.40	180 ± 20	18.8 ± 0.6
0.40[b]	200 ± 10	20.4 ± 0.4
1.0	132 ± 8	35.4 ± 0.7
4.0	70 ± 10	82 ± 6

[a] Reactions were followed by O_2 consumption at air saturation (except as noted), 25 °C, pH 7.4, 50 mM MOPS-KOH, 69 mM KCl, and 0.1 mM DTT, with saturating NADH and camphor. Data were fitted to the Michaelis−Menten equation. [b] Extrapolated to infinite O_2 concentration. [c] Measured at saturation with 1 atm. O_2 rather than air.

For three of the measurements in Table 1, however, the O_2 concentration was varied, showing that the $[PdR]_{halfmax}$ increases when the concentration of O_2 is elevated above air saturation. This can be explained by a similar reasoning as for the increase in $[PdR]_{halfmax}$ with increasing P450cam. As will be shown (Figure 2), the $K_m(O_2)$ for P450cam increases with Pdx, such that P450cam is not fully saturated with O_2 under air at the highest concentrations of Pdx. The effect of O_2 on $[PdR]_{halfmax}$ is very small at the lower concentrations of Pdx but produces as much as a 50% increase at 8 μM Pdx. For this reason, in studies where O_2 was varied, saturating concentrations of PdR were taken to be greater than 20 times the $[PdR]_{halfmax}$ value measured in air when [Pdx] was greater than 4 μM and to be 5−20 times the $[PdR]_{halfmax}$ measured at air when [Pdx] was 4 μM and below.

To demonstrate that all the Pdx was kept in its reduced form when PdR is saturating, UV−vis spectra were taken during a reaction in the steady state at a Pdx concentration twice as high as that employed in PdR and O_2 variation studies. At a saturating concentration of PdR, the spectrum of the reaction mixture in the steady state (Figure 1) looks very similar to the spectrum of Pdx after reduction by NADH and PdR. Therefore, a saturating concentration of PdR maintains all of the Pdx in its reduced state during turnover, even at this high Pdx concentration. Upon depletion of all NADH, the Pdx returns to its oxidized state as judged by the reappearance of the oxidized Pdx visible spectrum (not shown). As a control, Figure 1 shows that most of the Pdx is in the oxidized state during turnover with subsaturating PdR.

Dependence of the Apparent k_{cat} and $k_{cat}/K_m(O_2)$ on Pdx and PdR Concentrations. Using the previously determined concentrations of PdR required for saturation, it was possible to determine the steady-state kinetic parameters by varying the O_2 concentration at defined concentrations of Pdx^r. Figure 2 shows that both apparent k_{cat} and apparent $k_{cat}/K_m(O_2)$ vary hyperbolically with the concentration of Pdx^r. However, much lower concentrations of Pdx^r are required to saturate $k_{cat}/K_m(O_2)$ than k_{cat}. This indicates that the apparent $K_m(O_2)$ also changes with the concentration of Pdx, varying from 75 μM at the highest concentrations of Pdx^r to 20 μM at the lowest Pdx^r concentration employed in this series of experiments (0.25 μM). Table 2 summarizes the limiting kinetic parameters from fitting the data in Figure 2 to eq A.2.

As a clarification, in this paper, Pdx^r is considered as a substrate for P450cam since Pdx is typically at 10−1000-fold higher concentration than P450cam. The terms apparent k_{cat}, $K_m(O_2)$, and $k_{cat}/K_m(O_2)$ refer to those kinetic parameters derived from a fit to the Michaelis−Menten equation at a fixed, finite concentration of Pdx^r. The true kinetic constants are derived from a fit to eq A.2, where k_{cat} represents the rate with Pdx, O_2, and PdR saturating, and $k_{cat}/K_m(O_2)$ and $K_m(O_2)$ are at saturating Pdx and PdR. In all cases, camphor and NADH are also saturating.

A similar set of experiments was carried out with the wild type P450cam (lacking the $(His)_6$ tag), and the steady-state kinetic parameters are included in Table 2. The similarity of the parameters indicates that the N-terminal $(His)_6$ tag does not interfere with the reactivity of P450cam toward Pdx or O_2. This is consistent with the proposal that the binding site for Pdx is on the side opposite the N-terminus of P450cam (*35*, *36*).

The value of the apparent $k_{cat}/K_m(O_2)$ was also investigated as a function of the concentration of PdR at constant concentrations of 0.40 μM Pdx and 30 nM P450cam. The resulting data, plotted in Figure 3 in double reciprocal fashion, are parallel, indicating that $k_{cat}/K_m(O_2)$ is independent of the concentration of PdR. The movement of the *x*-intercept of the double reciprocal plot away from the origin as the concentration of PdR decreases shows how the apparent $K_m(O_2)$ decreases as the ratio of PdR to P450cam is decreased. A similar trend was noted in the mitochondrial steroid hydroxylase system in that the K_m for cholesterol was lowered upon decreasing the ratio of adrenodoxin reductase to P450scc (*37*).

Variation of P450cam and PdR Concentrations. Two studies have noted previously that, when holding the concentrations of Pdx and PdR constant, the observed rate depends hyperbolically on the concentration of P450cam (*20*, *38*). A similar phenomenon has been described in the mitochondrial steroid hydroxylase system (*37*). In the current study, these experiments are expanded upon by varying the concentration of P450cam at several fixed concentrations of PdR. The results are presented in Table 3B. Importantly, the values for both V_{max} and $[P450]_{halfmax}$ vary linearly with the concentration of PdR. This mirrors the trend observed for variation of PdR at fixed P450cam concentrations shown in Table 3A. These results strongly suggested that the apparent V_{max} obtained from P450cam variation represents the rate of reduction of Pdx by PdR.

To confirm this assertion, the rate of electron transfer from PdR to Pdx was measured using cytochrome *c* as an alternate electron acceptor in place of P450cam. Under enzyme concentrations similar to those employed here, Roome and Peterson showed that the rate of reduction of cytochrome *c* by Pdx^r is much faster than that of reduction of Pdx by PdR (*15*). This indicates that the observed rate of ferrous cytochrome *c* formation represents the rate of Pdx reduction by PdR. At 12.5 nM PdR and 4.0 μM Pdx, the rate of

Table 2: Steady-State Kinetic Parameters for P450cam[a]

	k_{cat}[b] (s^{-1})	$k_{cat}/K_m(O_2)$[c] ($\mu M^{-1}\ s^{-1}$)	$k_{cat}/K_m(Pdx^r)$[d] ($\mu M^{-1}\ s^{-1}$)	$K_m(O_2)$[c] (μM)	$K_m(Pdx^r)$[d] (μM)	$K_i(Pdx^r)$ (μM)
$(his)_6$ P450cam	55 ± 1	0.72 ± 0.03	26 ± 1	77 ± 2	2.11 ± 0.06	0.38 ± 0.03
wild type P450cam	66 ± 3	0.79 ± 0.07	17 ± 1	83 ± 6	3.8 ± 0.3	0.70 ± 0.06

[a] Conditions as in Table 1 except the concentration of O_2 was varied, and PdR was saturating at all pairs of Pdx and P450cam concentrations employed. Data were fitted to eq A.2 in the Appendix. [b] At saturating Pdx^r and O_2. [c] At saturating Pdx^r. [d] At saturating O_2.

Table 3: Variation of the Concentration of P450cam and PdR[a]

(A) PdR Variation at Fixed P450cam Concentrations

[P450cam] (nM)	$[PdR]_{halfmax}$ (nM)	apparent V_{max} ($\mu M\ O_2$/min)
8.1	16 ± 2	17.5 ± 0.6
13	25 ± 3	28 ± 1
20	39 ± 6	48 ± 3
33	70 ± 10	82 ± 6
70	120 ± 30	160 ± 20

(B) P450cam Variation at Fixed PdR Concentrations

[PdR] (nM)	$[P450]_{halfmax}$ (nM)	apparent V_{max} ($\mu M\ O_2$/min)
12.5	6 ± 1	13.1 ± 0.7
25	11 ± 2	25 ± 2
50	22 ± 5	57 ± 6

[a] All reactions at 4 μM Pdx and air saturation. Other conditions as in Table 1.

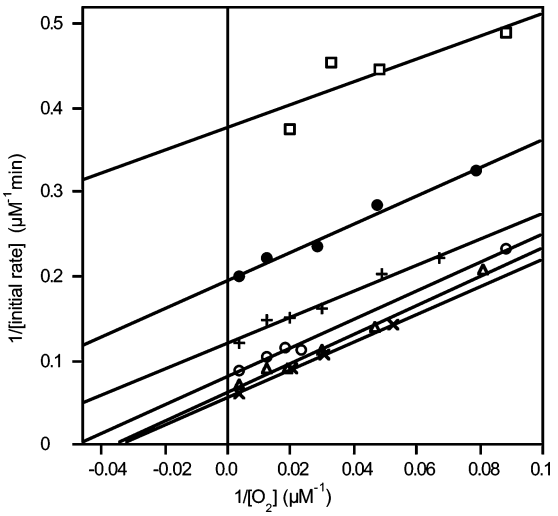

FIGURE 3: O_2 variation at fixed concentrations of PdR. Measurements of initial rates of O_2 consumption at 0.40 μM Pdx and 30.6 nM P450cam with varying concentrations of O_2. Other conditions as in Table 1. Concentrations of PdR are 1.0 μM (×), 0.50 μM (△), 0.25 μM (○), 0.13 μM (+), 0.063 μM (●), and 0.031 μM (□).

cytochrome *c* reduction was 23.5 ± 0.5 μM/min with saturating cytochrome *c*. At the same PdR and Pdx concentrations, the rate of O_2 consumption at saturating P450cam (the V_{max} in Table 3B) was 13.1 ± 0.7 μM/min. After correction for the fact that the passage of two electrons through Pdx to P450cam is required for consumption of a molecule of oxygen but only one electron is required to reduce cytochrome *c*, the rates are seen to be nearly identical.

Finally, a Scatchard plot, shown in Figure 4, was constructed from the kinetic data for variation of PdR at fixed P450cam concentrations. This plot was made to determine if the data could be construed as consistent with formation

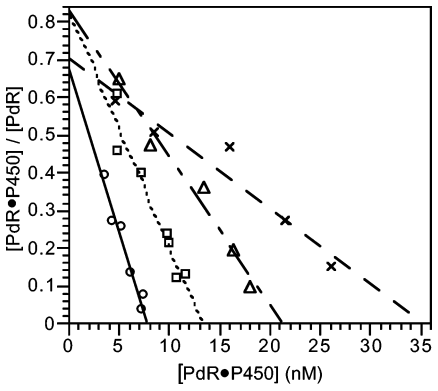

FIGURE 4: Scatchard analysis of kinetic data from PdR variation at fixed concentrations of P450cam. Reactions carried out at air saturation with 4 μM Pdx. Other conditions as in Table 1. Concentrations of P450cam are 8.1 nM (○), 13 nM (□), 20 nM (△), and 33 nM (×).

of a complex between PdR and P450cam, presumably bridged by Pdx, during the catalytic cycle. On the assumption that such a PdR/P450cam complex formed, rates were converted to the fraction of saturation of the P450cam enzyme (see Experimental Procedures). The Scatchard plot is expected to give a line with a slope of $-K_{eq}$ for the association of P450cam and PdR. From the plot in Figure 4, it is clear that the lines have different slopes as the concentration of P450cam is varied. Since a change in concentration of one of the components should not alter the equilibrium constant, these data are also incompatible with a binding equilibrium between PdR and P450cam.

The previous considerations impact the interpretation of steady-state kinetic data from experiments where the concentration of P450cam has been varied while Pdx and PdR are held constant. As mentioned previously, the apparent V_{max} values measured in such experiments represent the rate of reduction of Pdx by PdR (i.e., they are unrelated to electron transfer from Pdx to P450cam). When the reaction rate becomes independent of the concentration of P450cam but linearly dependent on PdR, PdR is the enzyme of interest. The value of $[P450cam]_{halfmax}$ has little to do with the binding of Pdx to P450cam but is, in reality, a condition-dependent empirical parameter that represents some balance between the rate of reduction of Pdx by PdR and the oxidation of Pdx by P450cam. The same can be said of the value of $[PdR]_{halfmax}$.

Impact of Partial O_2 Saturation on Measured Parameters. One important outcome of this study is the measurement of a $K_m(O_2)$ of 77 μM for P450cam at saturating Pdx^r. The concentration of dioxygen is only about 3-fold above the K_m when conditions of atmospheric oxygen (~258 μM in aqueous solution at 25 °C) are employed, meaning that reactions under air capture approximately 75% of the true k_{cat} when all other substrates are saturating. Mutation of P450cam or use of an alternate substrate could bring about

a significant change in $K_m(O_2)$. It may be advisable to compare the rates of reactions under air and 100% O_2 gas, provided that the contribution of the background reaction does not become too great at the elevated concentration of O_2.

In addition to being somewhat high as compared to air saturation, the apparent $K_m(O_2)$ decreases with the ratio of PdR to P450cam as shown in Figure 3. The effects of performing the experiments in Table 3, which involve varying the concentrations of PdR and P450cam at air saturation, are discussed here. An apparent $K_m(O_2)$ of 53 μM was measured at 4 μM Pdx with saturating PdR (Figure 2C). In the experiments in which P450cam is varied at a fixed concentration of PdR (Table 3B), the apparent $K_m(O_2)$ will be lowest at the highest concentrations of P450cam, indicating that atmospheric O_2 is sufficient to saturate the system. The values of apparent V_{max} in Table 3B would then not be affected by an increase in the concentration of O_2. However, at low concentrations of P450cam (hence high ratios of PdR to P450cam) the apparent $K_m(O_2)$ will approach 53 μM, indicating that the observed rate will only be approximately 80% of the true rate when O_2 is saturating. Making measurements at air saturation therefore introduces a systematic inflation of the observed values of $[P450]_{halfmax}$, although this is expected, at the most, to be ca. 20% (Table 3B). Additionally, the trends at the different concentrations of PdR should not be greatly affected by this systematic error. The same logic predicts that the apparent values of V_{max} and $[PdR]_{halfmax}$ (Table 3A) are subject to ca. <20% deflation relative to measurements at O_2 saturation. This is born out by the 17% increase in both $[PdR]_{halfmax}$ and apparent V_{max} in going from air saturation to infinite O_2 at 4 μM Pdx (Table 1A).

For steady-state kinetic studies in which the concentration of Pdx is varied at the atmospheric concentration of O_2, the rates measured at high concentrations of Pdx will be slightly underrepresented as compared to rates measured at low concentrations of Pdx due to the decrease in the apparent $K_m(O_2)$ with decreasing Pdx as shown in Figure 2C. Provided that PdR is kept saturating at all concentrations of Pdx employed, it should be possible to correct rates measured under atmospheric conditions to kinetic saturation with O_2 using apparent $K_m(O_2)$ values provided in Figure 2C.

Another parameter that varies with the concentration of Pdx is the amount of PdR required for saturation of the system. The $[PdR]_{halfmax}$ increases as the concentration of Pdx is lowered (Table 1). This could affect steady-state turnover studies in which the concentration of Pdx is varied at only one concentration of PdR. To alleviate this problem, the saturating concentration of PdR should be determined at the lowest concentration of Pdx to be employed. This will confirm that the rate is independent of the concentration of PdR, and hence, that Pdx stays in the reduced form under all conditions employed. If the fraction of Pdx in its reduced form varies in a series of experiments, then the meaning of the stated concentration of Pdx becomes unclear.

DISCUSSION

Kinetic Mechanism of Electron Transport from PdR to P450cam. As indicated by much previous work, a complex between Pdx^r, P450cam, and O_2 forms during turnover (*11*, *19*). This is supported by the present observation that $k_{cat}/K_m(O_2)$ changes with the concentration of Pdx^r as shown in Figure 2A. A ping-pong type mechanism where one substrate dissociates before the second binds would require that $k_{cat}/K_m(O_2)$ be independent of the Pdx^r concentration, but this is clearly not observed. Even further, the observed dependence requires that there be no irreversible step between Pdx^r and O_2 binding. A second piece of data gathered in this study is that $k_{cat}/K_m(O_2)$ is independent of the concentration of PdR (Figure 3). This indicates that, if there were a complex involving both PdR and O_2, an irreversible step would have to take place between their binding. These two pieces of data, along with experiments in which the concentrations of PdR and P450 are simultaneously varied, will be used to evaluate the three possible mechanisms for electron transport from PdR to P450cam. It should be noted that the mechanisms discussed here assume that, if a complex between PdR and P450cam existed, it would be bridged by Pdx. The formation of a very weakly bound PdR/P450cam complex has been demonstrated recently by optical detection with one of the proteins immobilized on a dextran coated surface (*23*), but this complex was much less tightly bound than the other productive protein−protein complexes studied.

The cluster mechanism where a PdR/Pdx/P450cam complex forms and survives for one or more turnovers can be discounted from the Pdx and PdR concentration dependencies of the apparent $k_{cat}/K_m(O_2)$ shown in Figures 2A and 3, respectively. The data would require that there be an irreversible step between the binding of PdR and O_2 but no irreversible steps between the binding of Pdx and O_2. This is clearly not possible given that both Pdx and PdR would be present in the complex during O_2 association in the cluster mechanism. The reported intracellular ratios of PdR, Pdx, and P450cam of 1:8:8 in *Pseudomonas putida* (*18*) also argue against an in vivo PdR/Pdx/P450cam complex that persists for multiple turnovers.

In contrast, formation of a transient PdR/Pdx/P450cam complex does fit with the observed trends in $k_{cat}/K_m(O_2)$. As depicted in Figure 5A, transfer of the first electron into P450cam occurs, followed by the binding of a reduced form of PdR (either the two- or one-electron reduced PdR, termed $PdR^{r/s}$) to the Pdx^{ox}/P450cam complex. This leads to Pdx^r and the oxidized form of PdR (now either the one-electron reduced or fully oxidized form, termed $PdR^{s/ox}$), which is released back into solution. Release of PdR fulfils the requirement for an irreversible step prior to O_2 binding. It would appear that this mechanism violates the requirement that all steps between Pdx and O_2 binding be reversible. However, the conditions under which $k_{cat}/K_m(O_2)$ is measured must be considered. In general, k_{cat}/K_m is determined by extrapolation to an infinitely low substrate concentration. Under conditions of low concentrations of dioxygen, the rate of O_2 binding to the Pdx^r/P450cam complex will be very slow as this is a second-order process. The Pdx^r bound to P450cam would have a chance to equilibrate with the free Pdx^r pool while it waits for O_2 to bind to continue the reaction. This is depicted in the off pathway equilibrium at the bottom of Figure 5A. At higher concentrations of O_2, the Pdx^r may not have time to exchange, distinguishing the transient cluster mechanism from the shuttle mechanism discussed in the following paragraph. Any variant of the transient cluster mechanism where PdR is released after the

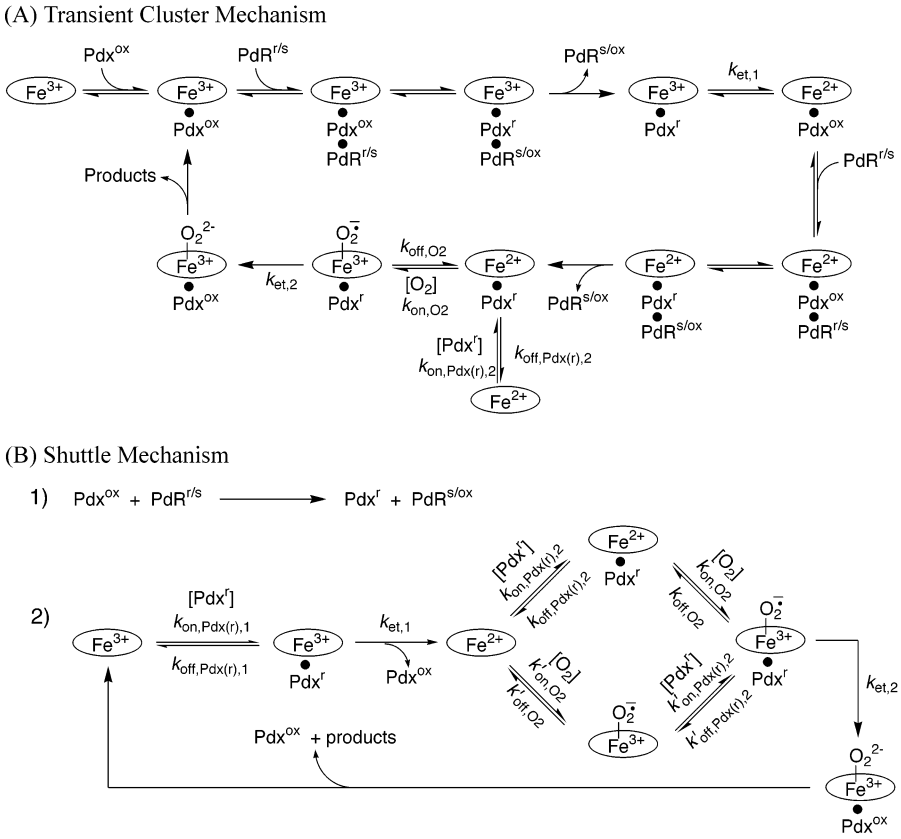

FIGURE 5: Two possible mechanisms for transfer of electrons from PdR to P450cam. The oval represents the porphyrin ring of camphor bound P450cam. Although not drawn, the substrate is saturating, and thus, bound to all forms of P450cam illustrated.

binding of O_2 or binds after O_2 but before the irreversible electron transfer and subsequent chemistry steps is ruled out by the observed independence of $k_{cat}/K_m(O_2)$ on the concentration of PdR.

The Pdx shuttle mechanism (Figure 5B) is the most consistent with the data presented here. That the apparent $k_{cat}/K_m(O_2)$ should be independent of the concentration of PdR in a shuttle mechanism requires some explanation since this type of situation is not usually discussed in terms of steady-state kinetics. Here, PdR behaves as the auxiliary enzyme in a coupled assay, serving to maintain a constant supply of Pdx^r to the P450cam during turnover. Varying the concentration of PdR serves only to modulate the fraction of Pdx that is in the reduced form during the steady state. The fraction of reduced Pdx depends on both the rate of reduction by PdR and the rate of oxidation by P450cam. Decreasing the concentration of PdR would tend to lower the fraction of Pdx that is Pdx^r, but the rate of reoxidation of Pdx by P450cam is dependent on the concentration of O_2. At the concentrations of O_2 from which $k_{cat}/K_m(O_2)$ is extrapolated, the rate of reaction of O_2 with P450cam is very low. Consequently, the rate of reoxidation of Pdx^r is very low. This means that at any finite concentration of PdR, all the Pdx will remain in the reduced form at infinitely low O_2 and the concentration of PdR will not affect the rate or $k_{cat}/K_m(O_2)$.

An important observation in support of the shuttle mechanism is the hyperbolic shape of plots of rate versus the concentration of P450cam at fixed concentrations of PdR, such that the plateau rate has become independent of the concentration of P450cam while remaining dependent on PdR. This pattern is fully consistent with the shuttle mechanism: at lower P450cam concentrations, the second reaction in Figure 5B (the oxidation of Pdx), limits the rate, while at high P450cam the rate-limiting step has been transferred to the first reaction in Figure 5B (the reduction of Pdx by PdR). This is confirmed by the observation that the rates of O_2 consumption with saturating P450cam and of cytochrome *c* reduction when this electron acceptor is substituted for P450cam are the same after the correction for an electron-transfer stoichiometry of 2:1 for these processes. The previous logic can be reversed to explain the hyperbolic shape of plots of rate versus PdR concentration at fixed P450cam concentrations.

In the course of these studies, we noted that hyperbolic plots could have arisen from the saturation of a complex under the transient cluster mechanism. Considering the case where a low concentration of P450cam is held fixed while PdR is varied, one might, for example, argue that the rate becomes independent of PdR when all the P450cam is bound into a complex at high PdR concentrations. To eliminate this ambiguity, experiments in which PdR was varied at multiple fixed concentrations of P450cam were further analyzed. As illustrated from the Scatchard plot in Figure 4, the data could not be modeled as arising from a PdR·P450cam complex. The aggregate data argue strongly for a shuttle mechanism in which PdR operates independent of a kinetically significant complex with P450cam.

Kinetic Order of Pdx^r and O_2 Binding to P450cam. According to the shuttle mechanism in Figure 5B, there are two possible binding pathways from reduced enzyme to the Pdx/P450cam/O_2 ternary complex. One way to assess the

degree to which binding of Pdx^r and O_2 are ordered or random is to examine the magnitude of $k_{cat}/K_m(Pdx^r)$ versus $k_{cat}/K_m(O_2)$ determined at saturating $[O_2]$ and $[Pdx^r]$, respectively.

The parameter $k_{cat}/K_m(O_2)$ includes all steps from O_2 binding up to the first irreversible step. This number can be compared with the rate constant for O_2 binding to P450cam, which sets the upper limit for $k_{cat}/K_m(O_2)$. Measurements of the rate constant for O_2 addition to the camphor-bound, ferrous P450cam are 7.7×10^5 M^{-1} s^{-1} at 4 °C (*5*) measured by stopped-flow and 17×10^5 M^{-1} s^{-1} at 25 °C (*14*) measured by temperature jump. Although the previous measurements were made in the absence of Pdx, it may be expected that the O_2 binding rate constant is similar in its presence (*19*). The value of $k_{cat}/K_m(O_2)$ measured in the present study is 7.2×10^5 M^{-1} s^{-1} at 25 °C (Table 2). This is slower than the previous measurements of the O_2 binding rate constant, suggesting that one or more steps beyond O_2 binding contribute to $k_{cat}/K_m(O_2)$. These steps are expected to include the long-range electron transfer from Pdx^r to the O_2 bound ferrous P450cam, indicated as $k_{et,2}$ in Figure 5B.

In contrast, the value of $k_{cat}/K_m(Pdx^r)$ is close to the previously measured values of the rate constant for Pdx^r binding to the camphor-bound, ferric P450cam. This binding rate constant has been evaluated by fits to measurements of the rate of Pdx to P450cam electron transfer as a function of Pdx concentration. Measurements are $\sim 2 \times 10^7$ M^{-1} s^{-1} at 10 °C (*10*) and 1.8×10^7 M^{-1} s^{-1} at 20 °C (*39*) for Pdx^r binding during the first of the electron transfers in the catalytic cycle. There is one estimate of the rate constant for the association of Pdx^r with the oxygen bound form of P450cam of $> 1.7 \times 10^7$ M^{-1} s^{-1} at 4 °C (*12*). The value of $k_{cat}/K_m(Pdx^r)$ measured in the present study is 2.6×10^7 M^{-1} s^{-1} at 25 °C (Table 2), which is quite similar to the measurements of the binding rate constants given the lower temperatures and somewhat different buffer conditions. Because Pdx could potentially bind twice in the catalytic cycle, $k_{cat}/K_m(Pdx^r)$ is a complicated parameter. However, since binding of Pdx^r to both the ferrous and O_2 bound forms of the P450cam are similar to $k_{cat}/K_m(Pdx^r)$, it appears that $k_{cat}/K_m(Pdx^r)$ is limited by one or both of the Pdx^r binding events and not by subsequent chemical steps.

The previous analyses indicate that Pdx^r is fully committed to catalysis once it has bound, whereas O_2 may undergo several cyles of dissociation and rebinding prior to $k_{et,2}$. In this case, $k_{off,O_2} > k_{off,Pdx(r),2}$ and the kinetic pathway for formation of Pdx/P450cam/O_2 is preferred ordered with the addition of Pdx^r preceding that of O_2 (upper pathway in Figure 5B).

Pdx Dependence of Steady-State Parameters. An expression for the apparent $k_{cat}/K_m(O_2)$ as a function of Pdx^r has been derived from eq A.2 (see Appendix) by substituting the definitions of the kinetic parameters in eqs A.3 to A.6, eq 6, and allowing the concentration of O_2 to approach zero

$$\left(\frac{k_{cat}}{K_{m,O_2}}\right)^{app} = \frac{\dfrac{k_{et,2}k_{on,O_2}}{k_{et,2} + k_{off,O_2}}[Pdx^r]}{\dfrac{k_{off,Pdx(r),2}}{k_{on,Pdx(r),2}} + [Pdx^r]} \quad (6)$$

The resulting relationship describes the hyperbolic curve shown in Figure 1A. The concentration of Pdx^r where the apparent $k_{cat}/K_m(O_2)$ is half of its maximum value is given by the ratio $k_{off,Pdx(r),2}/k_{on,Pdx(r),2}$. This ratio corresponds to the dissociation constant for Pdx^r binding to the camphor-bound, ferrous form of P450cam and is mathematically equivalent to the $K_i(Pdx^r)$ in the case that O_2 binds after Pdx^r. Previously, the K_D of the complex between the reduced forms of the two proteins was measured to be 0.49 μM at 10 °C by Sligar and Gunsalus using a fluorophore derivatized P450cam (*40*), while the $K_i(Pdx^r)$ in Table 2 shows a value of 0.38 μM. Although a random component cannot be rigorously excluded, the similarity of the kinetically determined dissociation constant to the previously measured K_D provides support for a mechanism in which Pdx^r binds to P450cam before O_2 (upper branch of Figure 5B).

Figure 2 shows that the apparent k_{cat} has a different Pdx^r dependence than does the apparent $k_{cat}/K_m(O_2)$. The hyperbolic curve in Figure 2B can be described for the shuttle mechanism using the preferred upper pathway for O_2 in Figure 5B

$$(k_{cat})^{app} = \frac{\dfrac{k_{et,1}k_{et,2}}{k_{et,1} + k_{et,2}}[Pdx^r]}{K_{m,Pdx^r} + [Pdx^r]} \quad (7)$$

where eq 7 derives from eq A.2 by extrapolation to infinite concentration of O_2. The expression for $K_m(Pdx^r)$ is complex, as shown in eq A.6. In contrast to the apparent $k_{cat}/K_m(O_2)$, the concentration of Pdx^r where the apparent k_{cat} is half of its maximal value does not describe a K_D for complex formation, involving instead steps from both Pdx^r binding and subsequent electron transfer (see Appendix).

Conclusions. The data presented here show that the hyperbolic curvature of the observed rate versus the P450cam concentration at a fixed concentration of PdR is due to a change in rate limiting step rather than a binding event. This is inconsistent with a mechanism where electrons are transported from PdR to P450cam through the formation of a PdR/Pdx/P450cam complex. The data indicate that Pdx acts as a freely diffusible shuttle for electrons and that the rate is limited by the reduction of Pdx by PdR at high ratios of P450cam to PdR and by the reoxidation of Pdx by P450cam at high ratios of PdR to P450cam.

The magnitude of $k_{cat}/K_m(Pdx^r)$ is close to the previously measured rate constant for Pdx^r association with P450cam, showing that binding controls this parameter. By contrast, $k_{cat}/K_m(O_2)$ appears smaller than previous measurements of the O_2 association rate constant, suggesting that at least one step beyond O_2 binding, presumably electron transfer, contributes to this steady-state kinetic parameter. This leads to the conclusion of a higher rate of dissociation of O_2 than Pdx^r from the enzyme ternary complex, and hence, a preferred ordered kinetic pathway in which O_2 binds to a preformed Pdx^r/P450cam complex. This is supported by the finding that a kinetically obtained value of $K_i(Pdx^r)$ matches a previous measurement of the K_D for this complex. For the future, the magnitude of the O-18 kinetic isotope effects, which can indicate the degree of commitment of the oxygen bound P450cam intermediate to catalysis, is expected to provide further insight into the proposed kinetic scheme. Last, the availability of values of $K_m(O_2)$ as a function of the

degree of saturation with both Pdx and PdR allows for the correction of rates measured at atmospheric O_2 to kinetic saturation with this substrate.

APPENDIX

Derivation and Interpretation of Steady-State Rate Expressions. A simplified kinetic scheme for the shuttle mechanism with O_2 binding after Pdx^r (as in the upper branch of Figure 5B) is given in the following scheme:

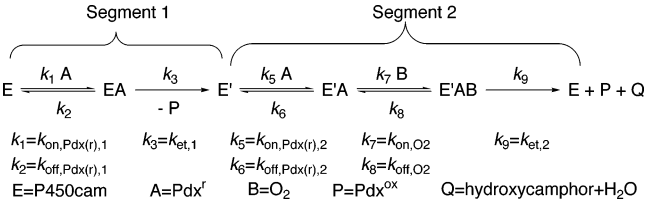

The scheme includes a key to link each numbered rate constant used here to the corresponding descriptive name in Figure 5B and the Discussion. The mechanism presented here can be thought of in two sections—a single substrate reaction (involving rate constants k_1-k_3) followed by a bisubstrate steady-state ordered reaction (involving rate constants k_5-k_9). The electron-transfer steps, k_3 and k_9, are written as irreversible because they are followed by the release of Pdx^{ox} as required by the shuttle mechanism. The product release steps could be included but are not shown explicitly here because there is no evidence that they are slower than the electron transfers. This mechanism takes the same form as the uni uni bi uni ping pong mechanism (*31*), but the rate expression is altered from its normal form because Pdx^r binds twice. Using Cleland's method of net rate constants (*41*), we obtain

$$\frac{v}{[E]_T} = \frac{1}{\dfrac{1}{\dfrac{k_1[A]k_3}{k_2+k_3}} + \dfrac{1}{k_3} + \dfrac{1}{\dfrac{k_5[A]k_7[B]k_9}{k_6(k_8+k_9)+k_7[B]k_9}} + \dfrac{1}{\dfrac{k_7[B]k_9}{k_8+k_9}} + \dfrac{1}{k_9}} \quad (A.1)$$

where v is the observed rate, and $[E]_T$ represents the total concentration of P450cam. This expression can be rearranged to yield

$$\frac{v}{[E]_T} = \frac{k_{cat}[A][B]}{K_{i,A}K_{m,B} + K_{m,B}[A] + K_{m,A}[B] + [A][B]} \quad (A.2)$$

where

$$k_{cat} = \frac{k_3k_9}{k_3+k_9} \quad (A.3)$$

$$K_{i,A} = \frac{k_6}{k_5} \quad (A.4)$$

$$K_{m,B} = \left(\frac{k_8+k_9}{k_7}\right)\left(\frac{k_3}{k_3+k_9}\right) \quad (A.5)$$

$$K_{m,A} = \frac{\left(\dfrac{k_2+k_3}{k_1}\right)k_9 + \left(\dfrac{k_9}{k_5}\right)k_3}{k_3+k_9} \quad (A.6)$$

Eq A.2 has the same form as the rate expression for an ordered bi bi system (*31*). Because the two A binding events are separated by an irreversible step, no terms involving $[A]^2$ are in the rearranged eq A.2. The difference between eq A.2 and the rate equation for a typical steady-state ordered mechanism (*31*) is in the definitions of k_{cat}, $K_{m,A}$, and $K_{m,B}$. The definition of $K_{i,A}$ is unchanged. The $K_{m,B}$ contains a term with its usual meaning, $(k_8 + k_9)/k_7$, but this is diminished by a term describing the extent to which the second electron-transfer limits k_{cat} (i.e., $k_3/(k_3 + k_9)$).

The $K_{m,A}$ is a complicated term that combines elements from both segments of the reaction. The term $(k_2 + k_3)/k_1$ would be the $K_{m,A}$ calculated for the first segment only, while the $K_{m,A}$ would be k_9/k_5 if only the steps after the first electron transfer were considered. Eq A.6 shows that the $K_{m,A}$ combines these two individual K_m expressions from the first and second reactions and weights them according to the electron-transfer rate constant for the opposite segment. The value of $K_{m,A}$ (i.e., $K_m(Pdx^r)$) should not be taken as an estimate of K_D or even as a composite of dissociation constants for the first and second reaction. The contribution of the second segment (k_9/k_5) contains no term for the release of substrate A because the intermediate E′A is trapped by saturating substrate B in the sequential ordered mechanism. As indicated in the Discussion, the dissociation of Pdx^r is slower than the rate of electron transfer. This indicates that the contribution of the first segment ($(k_2 + k_3)/k_1$) will not approximate a K_D either. Eqs A.1 to A.6 (and eqs 6 and 7) only apply when PdR is saturating. Otherwise, the Pdx^{ox} concentration will not be zero, even under initial conditions.

ACKNOWLEDGMENT

We would like to acknowledge Prof. Dexter Northrop (University of Wisconsin, Madison) and Dr. Julia Thrower (University of California, Berkeley) for valuable comments on the manuscript.

REFERENCES

1. Mueller, L. J., Loida, P. J., and Sligar, S. G. (1995) in *Cytochrome P450: Structure, Mechanism, and Biochemistry* (Ortiz de Montellano, P. R., Ed.) pp 83−124, Plenum Press, New York.
2. Makris, T. M., Davydov, R., Denisov, I. G., Hoffman, B. M., and Sligar, S. G. (2002) *Drug Metab. Rev. 34*, 691−708.
3. Bangcharoenpaurpong, O., Rizos, A. K., Champion, P. M., Jollie, D., and Sligar, S. G. (1986) *J. Biol. Chem. 261*, 8089−8092.
4. Davydov, R., Makris, T. M., Kofman, V., Werst, D. E., Sligar, S. G., and Hoffman, B. M. (2001) *J. Am. Chem. Soc. 123*, 1403−1415.
5. Peterson, J. A., Ishimura, Y., and Griffin, B. W. (1972) *Arch. Biochem. Biophys. 149*, 197−208.
6. Sharrock, M., Debrunner, P. G., Schulz, C., Lipscomb, J. D., Marshall, V., and Gunsalus, I. C. (1976) *Biochim. Biophys. Acta 420*, 8−26.
7. Harris, D., Loew, G., and Waskell, L. (1998) *J. Am. Chem. Soc. 120*, 4308−4318.
8. Ogliaro, F., de Visser, S. P., Cohen, S., Sharma, P. K., and Shaik, S. (2002) *J. Am. Chem. Soc. 124*, 2806−2817.
9. Hintz, M. J., and Peterson, J. A. (1981) *J. Biol. Chem. 256*, 6721−6728.
10. Hintz, M. J., Mock, D. M., Peterson, L. L., Tuttle, K., and Peterson, J. A. (1982) *J. Biol. Chem. 257*, 14324−14332.

11. Brewer, C. B., and Peterson, J. A. (1986) *Arch. Biochem. Biophys. 249*, 515−521.
12. Brewer, C. B., and Peterson, J. A. (1988) *J. Biol. Chem. 263*, 791−798.
13. Gerber, N. C., and Sligar, S. G. (1992) *J. Am. Chem. Soc. 114*, 8742−8743.
14. Tyson, C. A., Lipscomb, J. D., and Gunsalus, I. C. (1972) *J. Biol. Chem. 247*, 5777−5784.
15. Roome, P. W., and Peterson, J. A. (1988) *Arch. Biochem. Biophys. 266*, 41−50.
16. Lambeth, J. D., Seybert, D. W., and Kamin, H. (1979) *J. Biol. Chem. 254*, 7255−7264.
17. Hara, T., Koba, C., Takeshima, M., and Sagara, Y. (2000) *Biochem. Biophys. Res. Commun. 276*, 210−215.
18. Roome, P. W., Jr., Philley, J. C., and Peterson, J. A. (1983) *J. Biol. Chem. 258*, 2593−2598.
19. Pederson, T. C., Austin, R. H., and Gunsalus, I. C. (1977) in *Microsomes and Drug Oxidations: Prodeedings of the Third International Symposium* (Ullrich, V., Roots, I., Hildebrandt, A., Estabrook, R. W., and Conney, A. H., Eds.) pp 275−283, Pergamon Press, New York.
20. Holden, M., Mayhew, M., Bunk, D., Roitberg, A., and Vilker, V. (1997) *J. Biol. Chem. 272*, 21720−21725.
21. Sibbesen, O., De Voss, J. J., and Ortiz de Montellano, P. R. (1996) *J. Biol. Chem. 271*, 22462−22469.
22. Aoki, M., Ishimori, K., Fukada, H., Takahashi, K., and Morishima, I. (1998) *Biochim. Biophys. Acta 1384*, 180−188.
23. Ivanov, Y. D., Kanaeva, I. P., Karuzina, I. I., Archakov, A. I., Hoa, G. H., and Sligar, S. G. (2001) *Arch. Biochem. Biophys. 391*, 255−264.
24. Aoki, M., Ishimori, K., Morishima, I., and Wada, Y. (1998) *Inorg. Chim. Acta 272*, 80−88.
25. Peterson, J. A. (1971) *Arch. Biochem. Biophys. 144*, 678−693.
26. Auclair, K., Moënne-Loccoz, P., and Ortiz de Montellano, P. R. (2001) *J. Am. Chem. Soc. 123*, 4877−4885.
27. Lipscomb, J. D., Harrison, J. E., Dus, K. M., and Gunsalus, I. C. (1978) *Biochem. Biophys. Res. Commun. 83*, 771−778.
28. Gunsalus, I. C., and Wagner, G. C. (1978) *Methods Enzymol. 52*, 166−188.
29. De Voss, J. J., Sibbesen, O., Zhang, Z., and Ortiz de Montellano, P. R. (1997) *J. Am. Chem. Soc. 119*, 5489−5498.
30. Koo, L. S., Immoos, C. E., Cohen, M. S., Farmer, P. J., and Ortiz de Montellano, P. R. (2002) *J. Am. Chem. Soc. 124*, 5684−5691.
31. Segel, I. H. (1993) *Enzyme Kinetics*, John Wiley & Sons, New York.
32. Cleland, W. W. (1979) *Methods Enzymol. 63*, 103−138.
33. Scatchard, G. (1949) *Ann. N. Y. Acad. Sci. 51*, 660−672.
34. Cornish-Bowden, A. (1995) *Fundamentals of Enzyme Kinetics*, revised ed., Portland Press, London.
35. Roitberg, A. E., Holden, M. J., Mayhew, M. P., Kurnikov, I. V., Beratan, D. N., and Vilker, V. L. (1998) *J. Am. Chem. Soc. 120*, 8927−8932.
36. Pochapsky, T. C., Lyons, T. A., Kazanis, S., Arakaki, T., and Ratnaswamy, G. (1996) *Biochimie 78*, 723−733.
37. Tuckey, R. C., and Headlam, M. J. (2002) *J. Steroid Biochem. Mol. Biol. 81*, 153−158.
38. Di Primo, C., Sligar, S. G., Hoa, G. H., and Douzou, P. (1992) *FEBS Lett. 312*, 252−254.
39. Unno, M., Shimada, H., Toba, Y., Makino, R., and Ishimura, Y. (1996) *J. Biol. Chem. 271*, 17869−17874.
40. Sligar, S. G., and Gunsalus, I. C. (1976) *Proc. Natl. Acad. Sci. U.S.A. 73*, 1078−1082.
41. Cleland, W. W. (1975) *Biochemistry 14*, 3220−3324.

BI0356045